PHILOSOPHICAL TRANSACTIONS OF THE ROYAL SOCIETY A

Phil. Trans. R. Soc. A (2007) **365**, 1417–1433
doi:10.1098/rsta.2007.2024
Published online 11 April 2007

Supramolecular self-assembly codes for functional structures

By Liam C. Palmer[1], Yuri S. Velichko[2], Monica Olvera de la Cruz[2] and Samuel I. Stupp[1,2,3,*]

[1]*Department of Chemistry,* [2]*Department of Materials Science and Engineering, and* [3]*Department of Medicine, Northwestern University, Evanston, IL 60208, USA*

Small-molecule self-assembly has proven to be a rich field for the controlled synthesis of supramolecular objects with the size scale of polymers and interesting properties. Using several recent examples from our laboratory, we discuss the development of chemical structure codes for supramolecular self-assembly objects with defined shapes. The resulting materials formed by these objects are promising for electronic functions and biological functions for regenerative medicine.

Keywords: biomaterials; electronic materials; one-dimensional nanostructures; self-assembly

1. Introduction

Self-assembly 'spontaneously' creates functional structures or patterns with a significant order parameter out of disordered components. In order to avoid the trivial use of this important scientific term, spontaneity in self-assembly must imply that the components are 'designed' to achieve a specific structural outcome and their ordering involves little or no intervention by human beings or machines. Crystallization is the acme of self-assembly but in the present context, we only contribute to the science of self-assembly when molecular structure or atomic composition is used to predict or control the resulting crystal structure. There are many examples in the literature where this is indeed the objective, and we cite two excellent examples here (Sun *et al.* 2002; Ward 2005). The disorder-to-order transformations in self-assembly can occur at any length-scale (Whitesides & Grzybowski 2002). Reversibility in self-assembly should not be the defining feature of the disorder-to-order transformation—irreversible self-assembly under non-equilibrium conditions is no less interesting or useful. Similarly, with regard to the criterion of no human intervention, it is a matter of degree within the taxonomy of self-assembly processes. There will be processes that are 'templated' in a structural sense and others that will be externally 'directed' by forces applied by humans or machines. Self-assembling monolayers

* Author for correspondence (s-stupp@northwestern.edu).

One contribution of 12 to a Discussion Meeting Issue 'Supramolecular nanotechnology for organic electronics'.

of thiols on gold surfaces offer a very good example of templated self-assembly (Nuzzo *et al.* 1987; Porter *et al.* 1987; Bain & Whitesides 1988), whereas directed self-assembly could involve the application of external magnetic, electric or flow fields to induce or catalyse self-assembly (Messer *et al.* 2000; Smith *et al.* 2000; Whaley *et al.* 2000; Huang *et al.* 2001). It is interesting to consider how one might compute a figure of merit in the self-assembly processes that would measure the extent to which human intervention, templating or external energy are needed against the material value of the functions that the ordered structures or patterns produce. At the same time, the absolute merit of a process to be classified as 'self-assembly' could be judged by some 'index' that takes into account the magnitude of order parameters achieved in the final structure. Order parameters can be wide ranging in magnitude from the trivial to the remarkable. A set of macroscopic objects arranging into a pattern or structure has a trivial order parameter relative to the long-range periodicity of a macroscopic molecular crystal. In between, there are infinite possibilities such as the order parameters of liquid crystals, the order parameters of supramolecular nanostructures or the patterns of self-assembling block copolymers.

In molecular systems, supramolecular chemistry is the key in advancing the field of self-assembly (Hof *et al.* 2002; Lehn 2002; Mateos-Timoneda *et al.* 2004). Here, systematic and iterative studies on designed systems will be very useful to emulate the biological self-assembly in artificial systems. Our laboratory has had this focus over the past decade, seeking to develop self-assembly codes for function in macromolecular scales (Stupp *et al.* 1997; Hartgerink *et al.* 2001; Zubarev *et al.* 2001, 2006). In analogy to polymers, we define the scale as that of molecular assemblies in which the collective molar mass exceeds 10^4 daltons. The term 'code' implies that a specific type of structure defined by its architecture can be formed by design with diverse sets of molecules. Biology uses a spectacular set of codes to programme for structure and function. In the case of the globular protein code, folding of primary peptide sequences results in specific surface domains and hydrophobic pockets. In this paper, we comment on strategies developed in our laboratory that are emerging as codes to create very large assemblies of molecules with non-centrosymmetric shapes (like receptors in biology), ribbon-like strings that could have wire functions among others and cylindrical nanofibres that emulate biological fibrils of interest in cell signalling.

2. Supramolecular self-assembly at the macromolecular scale

One of the grand objectives in supramolecular chemistry is to create nanoscale structures with controlled size and shape and with a surface map of defined chemistry, essentially to emulate proteins in artificial systems. With function in mind, we are interested in this objective and also in the strategies needed to build lattices and patterns by self-assembly from these nanostructures. Going beyond nanostructures is important, since many of the potential functions of designed supramolecular systems may only emerge at these larger scales. A large number of low-molecular-weight molecules are obviously needed to create assemblies on the scale of macromolecules, approximately 10^4–10^7 Da. Current synthetic strategies to create very large controlled assemblies are inspired by previous examples of smaller systems, such as melamine–cyanurate spheres (Whitesides *et al.* 1991, 1995)

(diameter approximately 2.5 nm) and helicates (Koert *et al.* 1990; Hasenknopf *et al.* 1996, 1997). While these structures did not display any particular function, they established an important principle that small molecules can self-assemble into well-defined structures. There have been recent examples from us and others demonstrating interesting function in assemblies that reach into the macromolecular scale. For example, self-assembly causes a dramatic increase in the conductivity of Aida's hexabenzocoronene nanotubes (Hill *et al.* 2004) and Stupp's dendron-rodcoil ribbons (Messmore *et al.* 2004). Meijer has demonstrated both energy transfer (Hoeben *et al.* 2004) and photo-induced electron transfer (Schenning *et al.* 2002) in supramolecular assemblies of oligo(phenylenevinylene)s. These properties suggest great potential in photovoltaic and other devices. We have also found in our own work that appending biologically active functional groups to macroscale supramolecular structures has led to materials with interesting biological properties, particularly in unprecedented control over neural stem cell differentiation and in the rapid development of vascular tissue (Silva *et al.* 2004; Rajangam *et al.* 2006). The discovery of such functions makes sense, given the importance of surface- and interface-mediated interactions in biology.

In this article, we explore the notion of codes for supramolecular self-assembly of small molecules into nanostructures. These codes should be accessible to large sets of similar molecules to be useful, and their development needs to consider not only the attractive forces (hydrogen bonding, electrostatics and π-stacking) but also the nature of entropic penalties, repulsive interactions, cooperativity and external forces.

3. Entropy-limited finite crystallization

Nearly a decade ago, our group discovered that mushroom-shaped, non-centrosymmetric zero-dimensional nanostructures form spontaneously from molecules like **1a–c** (figure 1; Stupp *et al.* 1997). These molecules were designed to incorporate a flexible, oligomeric coil crystallizing segment and a rigid, aromatic rod-like segment. Approximately 100 of these rodcoil monomers come together by attractive interactions among rod segments leading to nanoscale crystallization. However, complete crystallization is frustrated by the repulsive steric forces among the non-crystallizable coil segments limiting the size of the aggregates. Thus, the rigid and flexible portions phase separate to create a nanocrystal covalently bonded to a nanoscale amorphous aggregate of flexible segments. The resulting organic nanoclusters (approx. 5 nm) are zero-dimensional, like quantum dots, but have a non-centrosymmetric polar shape. Molecular dynamics simulations showed that as the aggregation number increases, the splayed coils are more conformationally restricted as they seek to minimize steric repulsions (Sayar & Stupp 2001). Thus, the entropy of the coils appears to be integral to the restricted supramolecular growth (figure 2). This process can be imagined as a partial vitrification—a process that effectively leads to a glass–crystal graft.

These mushroom nanostructures were found to further assemble into layers with polar, non-centrosymmetric stacking (figure 3). Since the films lack an inversion centre, some unusual properties are observed. Rodcoil structures, with a

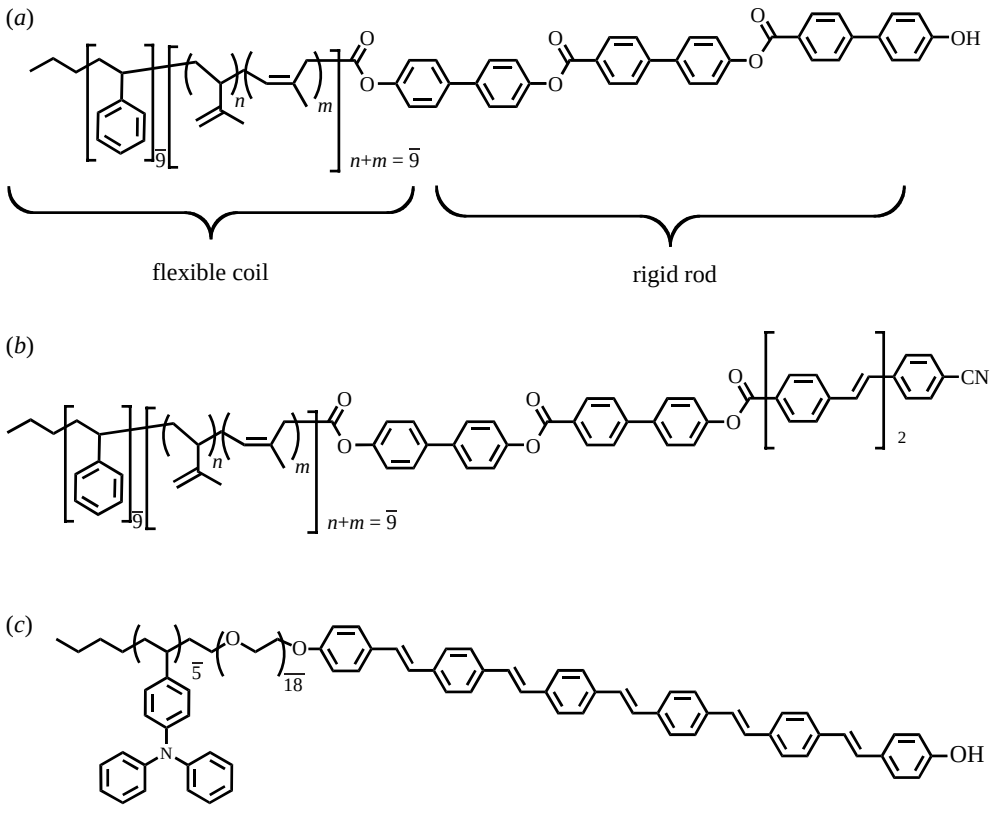

Figure 1. Chemical structure of the monomeric mushroom precursors (**1**).

polystyrene and polyisoprene coil, formed particularly regular nanostructures. Interestingly, cyano-substituted rodcoil **1b** assembles into macroscopic films with measurable piezoelectricity. The observed electromechanical properties result from interactions between the substrate and polar domains of the film (Pralle *et al.* 2000). Ordering within these films is further confirmed by small-angle X-ray scattering (SAXS) and second-harmonic generation (SHG; Tew *et al.* 1998). Profilometry studies show that these films can be thousands of layers thick (20–110 μm; Tew *et al.* 1998). Figure 4 explains the mechanism of the higher-order assembly and the resulting piezoelectric behaviour. Calculations indicate that a polar phase is only energetically possible for nanostructures, like the mushroom, in which the cross-section is comparable to their height (Sayar *et al.* 2003).

4. One-dimensional assemblies

One-dimensional (1D) assemblies are those that possess a single axis far longer than the others (by a factor of 100–1000 or greater). On the nanoscale, these types of structures (including nanotubes) exhibit a number of interesting properties, including potential for alignment, conductivity and biological interactions. As these 1D structures entangle, they behave like linear polymers and are able to entrap solvent molecules—macroscopically observed as a gel (Terech & Weiss 1997; Estroff & Hamilton 2004).

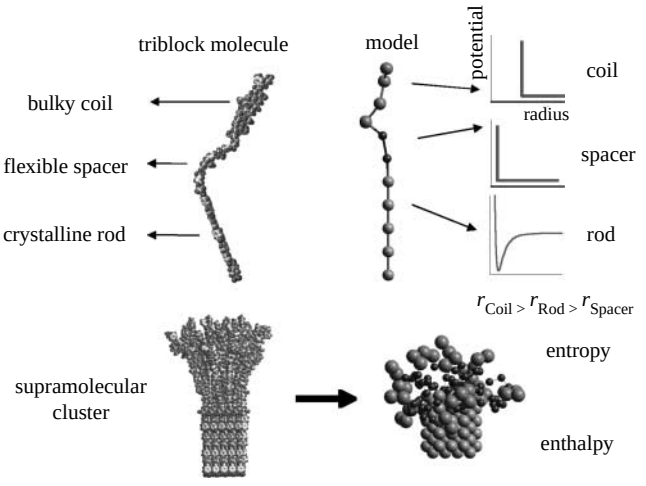

Figure 2. The model for the entropy-limited crystallization code involves crystallization of rod segments made up of structural units with radii that are smaller than those of structural units in bulky coil and spacer segments. At distances larger than those at which crystallized rod segments achieve their energy minimum due to crystallization, the bulky coil segments experience repulsive interactions. These repulsive interactions impose an entropic penalty on the cluster and growth of the unit stops creating a finite-sized supramolecular object.

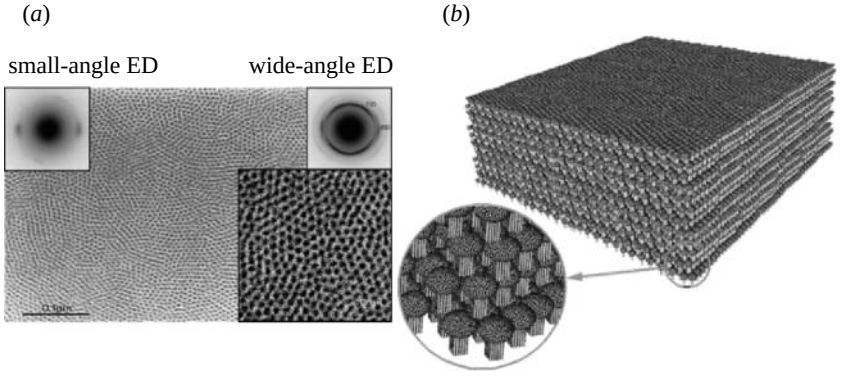

Figure 3. Ordering of the mushroom assemblies. (*a*) Electron micrograph and electron diffraction patterns (inset). (*b*) Schematic of the layering and polar ordering of the mushroom assemblies. The layered structure results in a hydrophilic and a hydrophobic plane at the top and bottom of the structure.

(*a*) *Code: packing controlled by nonlinear geometry*

The assembly of the rodcoil into mushroom-shaped assemblies inspired the design of other molecules. Structurally related to the mushroom precursor **1**, the dendron rodcoil (DRC) incorporates a dendritic block to one terminus of the rodcoil segment. DRC **2** was found to form a gel at concentrations as low as 0.2 wt % in dichloromethane (figures 5 and 6). Transmission electron microscopy (TEM) and atomic force microscopy (AFM) indicate the formation of high-aspect ratio supramolecular ribbons with widths approximately 10 nm and a thickness approximately 2 nm.

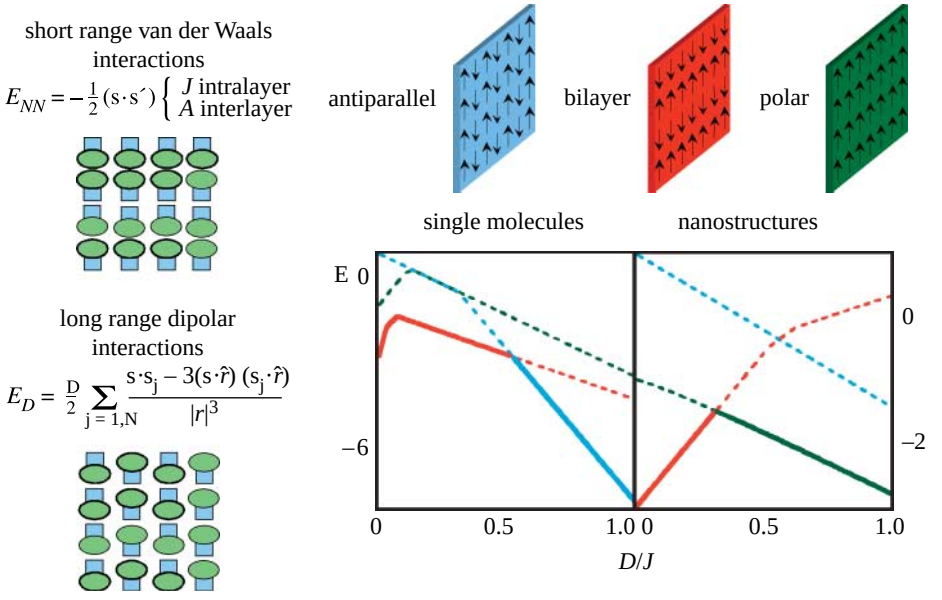

Figure 4. In the right hand side of the figure, arrows represent dipoles. Calculations indicate that a polar phase (shown in green) is only energetically possible for nanostructures, like the mushroom objects, in which the cross-section is comparable to their height. In contrast, for polar molecules in which the cross-section is much smaller than the length, the polar phase never becomes energetically favourable relative to centrosymmetric arrangements of the objects (blue and red). The parameter space explored by the calculations is the ratio D/J, which measures the coefficients for long-range dipolar and short-range van der Waals forces among the molecules.

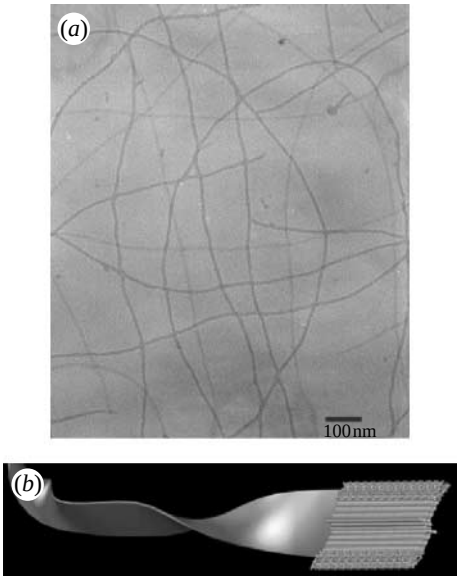

Figure 5. 1D assemblies of DRC molecules. (*a*) TEM microscopy of nanofibre structure. (*b*) Molecular graphics representation of the nanofibre ribbon. Adapted with permission from Zubarev *et al.* (2001).

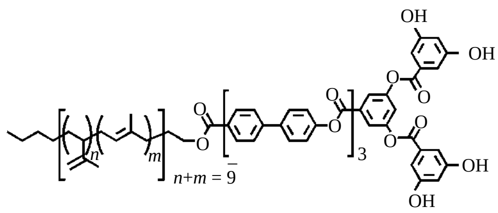

2

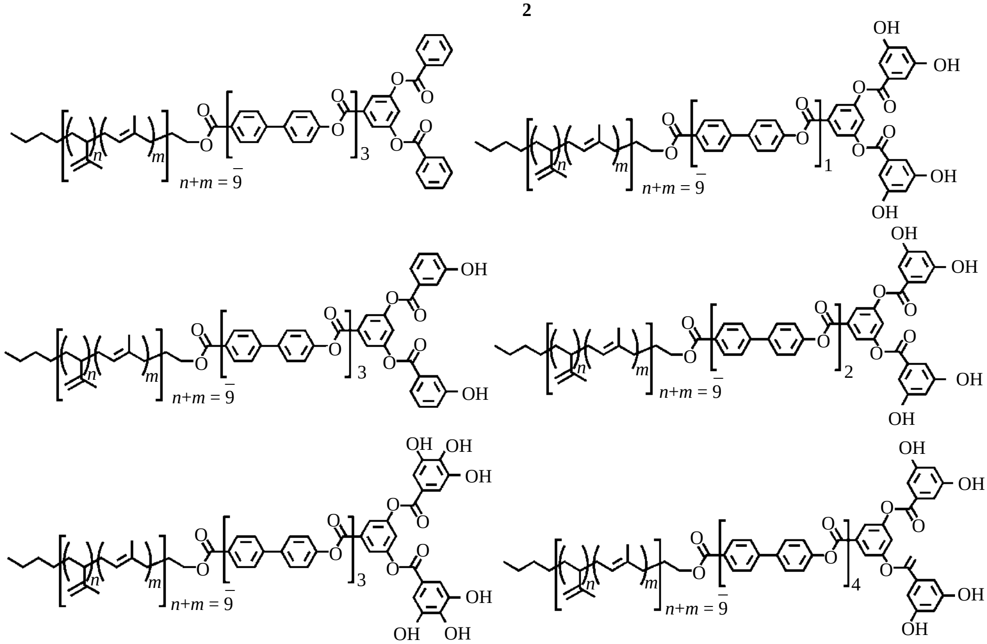

Figure 6. Chemical structures of DRC derivatives. Changes to the dendron portion (left) and changes to the length of the rod portion (right) are indicated in grey.

The monomeric structure that forms the supramolecular assembly is composed of three distinct structural elements: a dendritic headgroup (D) with hydrogen-bond functionality; a 'rod' (R) composed of rigid aromatic groups that aggregate or crystallize (by π–π stacking interactions and reduced conformational entropy, vide supra); and an oligo(isoprene) coil (C) that provides solubility. Each of these portions was systematically mutated to determine its relative importance in self-assembly (Zubarev *et al.* 2006).

(i) *Dendron*

The G1 DRC (e.g. **2**) forms ribbon assemblies with the dendrons forming head-to-head hydrogen bonds. Higher-generation dendrons such as G2–G4 afford only isolated aggregates. Presumably, the bulky size and shape of the dendron inhibit self-assembly (figure 7). In the absence of the dendritic segment, the molecules are no longer soluble.

The number of available hydrogen bonding groups also matters. Monomers with no hydroxyls give isotropic solutions; those with two hydroxyls do not form the ribbon assemblies and precipitate instead at room temperature

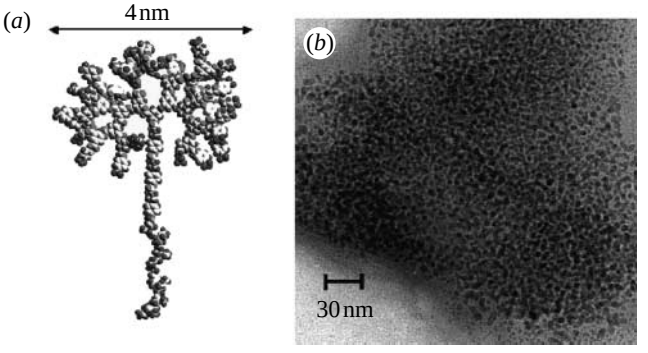

Figure 7. (*a*) Molecular model and (*b*) TEM image of dendron-rodcoil stained with OsO_4. The generation four-dimensional segment inhibits molecular aggregation and single molecules are visualized by TEM.

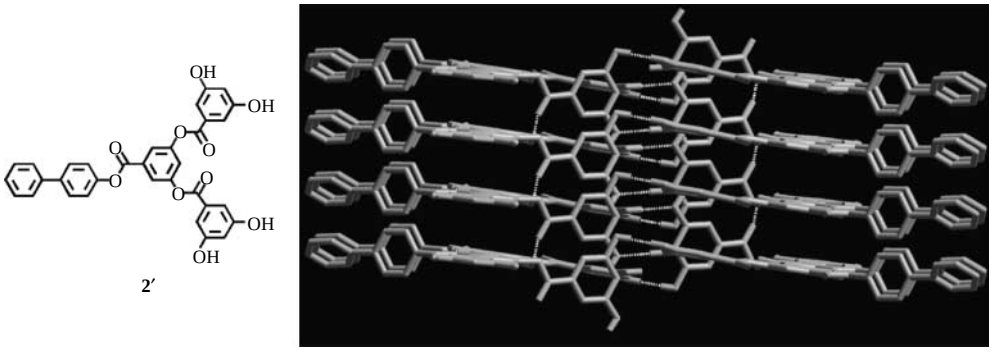

Figure 8. Compound **2′** crystallizes as a stack of cyclic tetramers. Hydrogen bonds between adjacent tetramers are indicated by dashed lines. Adapted with permission from Zubarev *et al.* (2001).

(figure 7). Compounds displaying four or six hydroxyls per monomer give purple gels from non-polar solvents. SAXS confirms that the crystalline order of the assembly increases with more hydrogen bonding groups (figure 8). This rigid portion also serves to offset some of the entropic cost of bringing together so many molecules.

To more precisely understand the interactions between the adjacent dendrons, a partial dendron-rod (**2′**) was prepared and crystallized (Zubarev *et al.* 2001). The dendrons form hydrogen cyclic tetramers through four hydrogen bonds. Eight additional hydrogen bonds hold adjacent tetramers together in a stack (figure 8).

(ii) *Rod*

A single biphenyl ester in the rod portion gives only a viscous, isotropic solution. As the rod portion is lengthened to two, three or four biphenyl esters, purple birefringent gels of increasing strength are obtained indicating the self-assembly of supramolecular ribbons (figure 4). Other rigid, aromatic groups besides oligophenylenes are also tolerated in the self-assembly (vide infra).

(iii) *Coil*

The incorporation of a coil segment offers solubility to DRC self-assembling molecules, but it is also important to use its architecture to prevent interdigitation among the hydrogen-bonded assemblies. In addition to the polyisoprene coil of compound **2**, the assembly also forms with a shorter, branched alkyl coil (vide infra) (Zubarev *et al.* 2001). Regardless of chemical composition, it was found that the length of coil should be at least on the order of the length of the rod block. Interestingly, diblock segments such as the one used in the mushroom aggregate inhibit the 1D self-assembly of the ribbon. This could be interpreted as the result of the entropic penalty described for the previous code.

The three components (dendron, rod and coil) of DRC molecules work in concert to provide the code for 1D self-assembly of ribbons. If any one of these units is of the wrong size, shape or chemical composition the code breaks down. When the code works experimentally, gels form and ^{1}H NMR reveals the broadening of the coil protons and complete loss of resonances (broadening to baseline) for the aromatic (dendron and rod) protons. The physical basis of this code is thought to be rooted in the nonlinear, rigid geometry of the functionalized D segments, which blocks many options for efficient packing of the molecules allowing only 1D assembly. However, as mentioned above, it is also important for the C segment to avoid the type of interdigitation among ribbons that would result in formation of a two-dimensional assembly. Again, a nonlinear geometry in the C segment helps as well. However, the role of the C segment may be secondary to that of the dendritic one since dense packing of the rigid RD segments entropically blocks the C interdigitation. We demonstrate below the validity of the code by providing examples of mutated structures that preserve these essential elements and provide access to interesting function.

Other rigid aromatic groups were introduced into the rod, including oligothiophenes, oligo(biphenyl ester)s and oligo(phenylenevinylene)s (Messmore *et al.* 2004). In the oligothiophene derivative **3**, self-assembly leads to three orders of magnitude increase in the conductivity of iodine-doped films (figure 9). This conductivity is in contrast to the biphenyl ester rods, which are completely insulating. It was also shown that electric field alignment of these supramolecular assemblies could be used to create arrays of self-assembled nanowires on a device substrate.

DRC **4** possessing a chiral coil was shown to self-assemble into ribbons of a prescribed handedness (Messmore & Stupp 2005; figure 10). This supramolecular chirality could be used as a potential chiral catalyst.

The DRC also was used as a template for the first reported synthesis of a nanohelical 1D cadmium sulphide nanostructure (Sone *et al.* 2002). By TEM, the mineralized helices showed widths of 35–100 nm, pitches of 60 nm and lengths of several micrometres. Unmineralized assembly of the same compound gave nanohelices with a 20 nm pitch, explaining its effectiveness as a template. The twisted as opposed to the flat architecture of the ribbon was induced using a semi-polar solvent as the medium of ribbon self-assembly. The DRC nanoribbons are also able to bind organic dyes and semiconductor nanoparticles. When mixed with ZnO nanocrystals, the assemblies were able to align parallel to the poling direction of an applied electric field (DC, 1500 V cm^{-1}; Li *et al.* 2003). The resulting material showed strongly anisotropic emission and ultraviolet lasing with a lower threshold compared with pure zinc oxide nanocrystals. Adding a small amount of

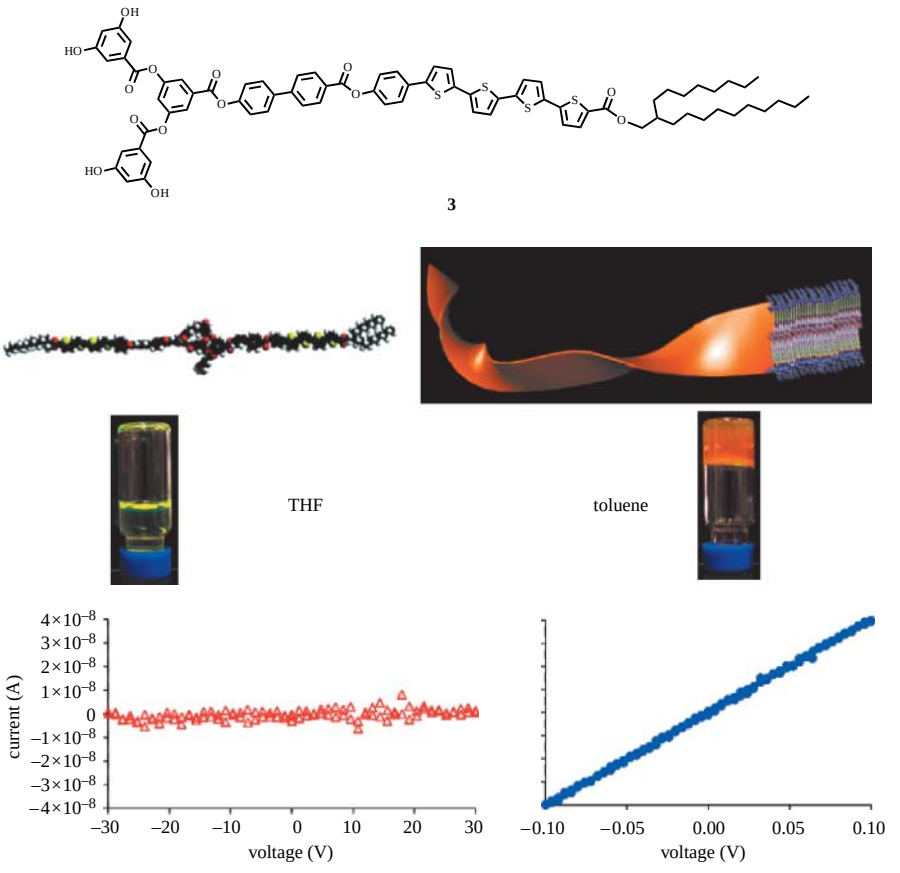

Figure 9. The conductivity of the oligothiophene DRC **3** increases from 8.0×10^{-8} S cm^{-1} in THF (left) to 7.9×10^{-5} S cm^{-1} in the assembled state (right). Reproduced with permission from Messmore *et al.* (2004).

DRC (0.1 wt %) to neat styrene monomer leads to a birefringent gel (Stendahl *et al.* 2002). After thermal polymerization, the dispersed material is still birefringent and has a 70% higher Charpy impact strength relative to polystyrene homopolymer. This demonstrates the possibility of using these 1D assemblies to modify significantly the mechanical properties of ordinary polymers. The very stable networks formed by these assemblies are likely to divert growing cracks and if the secondary bonds within them are broken they can easily heal.

(*b*) *Code: hydrophobic collapse of amphiphilic sheets*

Peptide amphiphiles (PA, e.g. **5**) were introduced as a novel class of molecules that self-assemble into 1D nanostructures (Hartgerink *et al.* 2001). The PA molecule consists of an unbranched alkyl or other single-chain hydrophobic moiety linked to an electrostatically charged peptide sequence (figure 11). When the peptide sequence includes amino acids with high β-sheet propensity, high aspect ratio cylindrical nanoscale fibres are observed. Screening of charged groups (by pH or ionic strength changes) results in a self-supporting gel as a

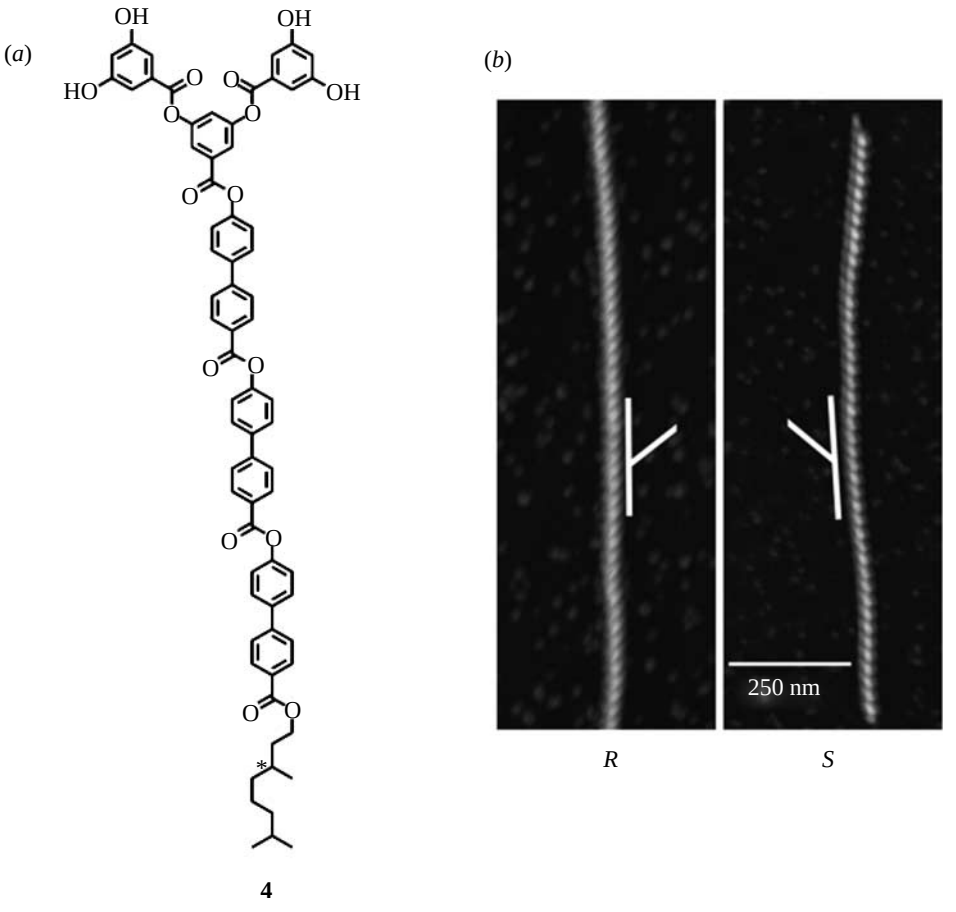

Figure 10. Chirality in the coil portion of **4** leads to a supramolecular chiral assembly with defined handedness that is directly observable by AFM. Switching the chirality of the indicated methyl group results in twisted ribbons, which are mirror images of each other. Reproduced with permission from Messmore & Stupp (2005).

result of the networks formed by these 1D assemblies. Self-assembly of PA molecules is further controlled by hydrophobicity of the alkyl tail and hydrogen bonding between adjacent peptides. The morphology of the PA assemblies has been characterized by transmission and scanning electron microscopy techniques (TEM and SEM), atomic force microscopy (AFM), circular dichroism (CD), nuclear magnetic resonance (NMR) and infrared (IR) spectroscopy (Behanna *et al.* 2005; Jiang *et al.* 2007).

The self-assembly is remarkably tolerant to changes to the peptide sequences as long as a robust β-sheet forming sequence is included. The formation of β-sheets blocks the formation of alternative aggregates, such as spherical micelles or layered structures even when molecules vary greatly in their shapes. Tsonchev *et al.* (2003, 2004) showed through calculations and Monte Carlo simulations that spherical micelles are preferred by tapered molecules. Israelachvili *et al.* (1976) has postulated that surfactants will aggregate into spheres, cylinders or layered assemblies depending on how tapered is the shape of molecules. Thus, we believe

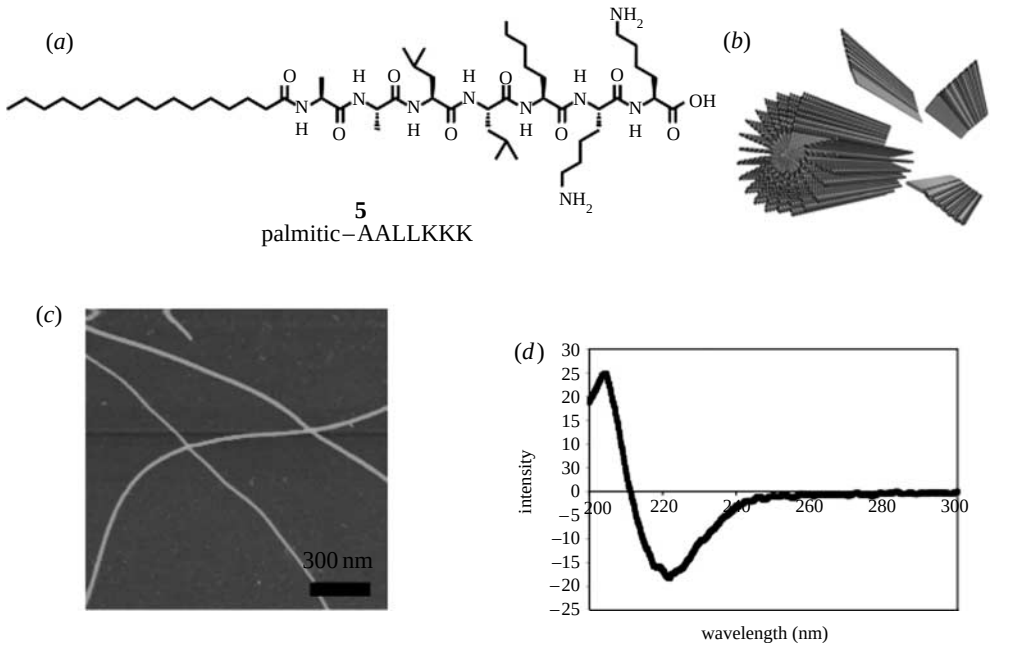

Figure 11. (*a*) Structure of a typical peptide-amphiphile monomer **5**, in this case displaying the bioactive epitope RGDS. (*b*) Schematic of cylinder formed from β-sheets. (*c*) AFM image showing nanofibres from a 1 : 1 mixture of palmitic-IEIE and palmitic-IKIK. (*d*) CD spectrum of palmitic-LLLGGKK indicating β-sheet formation.

the specific tendency of certain amino acid sequences to form β-sheets is the essence of this particular code which yields cylindrical aggregates in a very large set of molecules, which based on their architecture would have been expected to self-assemble into a large variety of shapes. Hartgerink recently showed with a series of alanine and *N*-methylated PA mutants that the β-sheet residues closest to the hydrophobic core—particularly the first four amino acids—are crucial for β-sheet assembly and for the versatile cylindrical structure (Paramonov *et al.* 2006). Supporting our proposed physical basis for this code, a PA was reported earlier by the group of M. Tirrell that was designed to produce alternative protein-like secondary structures, including α-helices and proline-helices (Fields *et al.* 1998; Yu *et al.* 1998) do not form high aspect ratio nanofibres, but can organize into two-dimensional assemblies.

The functional significance of this code lies in the ability of these cylindrical aggregates to display on their surfaces peptide-based biological signals perpendicular to their long axis in very high density. In fact, they can simultaneously display a very large diversity of biological signals without losing their cylindrical shape. In analogy to the DRC ribbons, this allows the 1D PA cylinders to create networks and therefore gel states that can be extremely useful *in vivo* or *in vitro* biological assays. Neural progenitor cells were encapsulated *in vitro* within a three-dimensional network of peptide amphiphile nanofibres presenting a high density of the neurite-promoting laminin epitope IKVAV (Silva *et al.* 2004). In this case, the gelation can be triggered by mixing cell suspensions in media with dilute aqueous solutions of the PA. The cells survive

the assembly of the nanofibres and were shown to induce the unprecedented rapid and selective differentiation of neural progenitor cells into neurons with minimal development of astrocytes. This rapid selective differentiation suggests their possible application in the treatment of spinal cord injury, stroke and other neurodegenerative diseases. A different PA was recently designed for its potential to bind heparin, a biopolymer known to bind angiogenic growth factors (Rajangam *et al.* 2006). Self-assembly leads to nanofibres that appear to orient the heparin for cell signalling. *In vivo*, nanogram quantities of the nanostructures and appropriate growth-factor proteins were sufficient to stimulate extensive new blood vessel formation. Rapid formation of new blood vessels could be extremely useful in regenerative medicine, particularly in the regeneration of heart muscle after infarct and also in the challenge of wound healing. Despite extensive experimental characterization, a detailed theoretical description of cylindrical PA assemblies in this code remains elusive. Here, we present a model of PA molecules and demonstrate the importance of hydrogen bonding and hydrophobic interactions in their self-assembly. For the sake of computational efficiency, we do not take into account the chemical structure of PA. Rather, we construct a coarse-grained model for the PA (Velichko *et al.* in preparation) using a united atom model; adjacent, chemically similar segments of the molecule are treated as a single effective unit (Allen & Tildesley 1987; Velichko *et al.* in preparation). For the purposes of the coarse-grained model, the PA is divided into three distinct units: hydrophobic (H); peptide (P); and epitope headgroup (E).

Hydrophobic (non-bonded) interactions between monomer units are described by the Morse potential (Allen & Tildesley 1987; Velichko *et al.* in preparation),

$$U_M(r_{ij}) = \varepsilon_{HH}\left[\exp\left(-2\alpha\frac{\Delta r_{ij}}{\sigma}\right) - 2\exp\left(-\alpha\frac{\Delta r_{ij}}{\sigma}\right)\right],$$

where ε_{HH} determines the depth of the potential well; σ is the diameter of the monomer unit; r_{ij} is the distance between i-th and j-th monomer units; and $\Delta r_{ij} = r_{ij} - \sigma$. The constant $\alpha = 24$ determines the shape of the potential and how fast it goes to zero. To maintain the distance between chemically connected monomer units and to prevent chains from crossing each other, we use a finitely extendable nonlinear elastic potential (Allen & Tildesley 1987).

Hydrogen bonding is frequently considered as an intermolecular force between two partial electric charges of opposite polarity. However, the hydrogen bond also involves a shared hydrogen atom and has partial covalent character. When the hydrogen bond is formed, the redistribution of the electron charge density restricts the possibility of forming additional bonds. Another important feature of the hydrogen bond is that the formation of the bond depends on the relative spatial distribution of atoms. We assume that each subunit P is capable of forming two sets hydrogen bonds (i.e. to each of the P subunits of adjacent monomer). Hydrogen bonding requires activation of the peptide before the formation of the bond described by the activation energy V_{a} and the intramolecular energetics V_{e} of the new bond. The activation energy depends on the orientation of the donor and acceptor groups. For the sake of simplicity, we use a two-state model to describe the activation of the monomer with the activation energy $V_{\mathrm{a}} = \varepsilon_\beta \cos(\theta_{ij})$, where θ_{ij} is an angle between donor and acceptor groups. When two monomer units are linked by a hydrogen bond, the

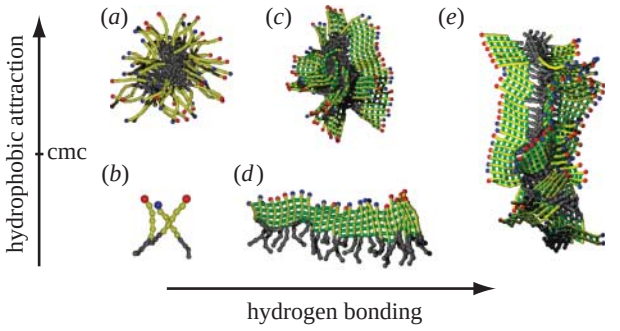

Figure 12. Snapshots of self-assembled peptide amphiphiles at different values of hydrogen-bond activation energy (a,b) $\varepsilon_A=0.0$, (c,d) $\varepsilon_A=2.0$ and (e) $\varepsilon_A=3.0$ and strength of hydrophobic attraction $(a,c$ and $e)$ $\varepsilon_H=3.0$ and (b,d) $\varepsilon_H=0.5$ in k_BT energy units. Hydrogen-bond activation energy ε_A is connected with an equilibrium constant $\varepsilon_A/k_BT=\log[k]$ of the hydrogen bonding reaction. Hydrogen bonding prevails over thermal fluctuations when ε_A is greater than k_BT and supports formation of long β-sheets. The hydrophobic groups are coloured grey, β-sheet forming peptides in yellow and the terminal epitopes are blue or red. Hydrogen bonds between epitopes of adjacent peptides are indicated in green.

bond is described as a regular chemical bond, albeit a rather weak one by covalent standards. The assembly of PA molecules into parallel β-sheets can be easily introduced into this model by defining corresponding values for dihedral angles of amides. The planar β-sheet structure is determined by an angular potential (bending energy of the β-sheet) applied to the angle formed by two hydrogen bonds. The energy of the new bond and the bending energy of the β-sheet constitute the intramolecular energetics V_e of the hydrogen bond.

A simulation was carried out within the framework of the mixed Monte Carlo–stochastic dynamics method (Chandler 1978; Leach 2001), which performs alternating stochastic dynamic and Monte Carlo steps. The stochastic dynamic step is performed in Cartesian space by solving Langevin's equations

$$m_i\frac{\mathrm{d}^2\boldsymbol{r}_i}{\mathrm{d}t^2}=-\frac{\partial U(\boldsymbol{r},t)}{\partial \boldsymbol{r}}-\gamma\frac{\mathrm{d}\boldsymbol{r}_i}{\mathrm{d}t}+\Gamma_i(t),$$

where m_i is the mass and $\boldsymbol{r}_i$ is the position vector of i-th monomer unit; $U(\boldsymbol{r},t)$ is the interaction potential affecting the monomer unit at a time t; the friction coefficient or damping constant $\gamma=1$ in reciprocal time units; and $\Gamma(t)$ is a stochastic force satisfying the conditions of Gaussian white noise. In our simulation, an additional Monte Carlo step was performed at each time-step to create or break hydrogen bonds. Formation of the bond was accepted according to the Metropolis criterion with a probability given by

$$\Pi^+=\frac{\mathrm{e}^{-\frac{Va+Ve}{k_BT}}}{1+\mathrm{e}^{-\frac{Va+Ve}{k_BT}}}>R,$$

where $0<R<1$ is a random number. The probability of breaking the hydrogen bond (Π^-) is taken to be $1-\Pi^+$ (figure 12).

The composition of the PA molecules and competition between different forces assist to break down the three-dimensional symmetry of molecular interactions and to guide aggregation into the observed cylindrical assemblies. The path to this structure has proven difficult to be determined experimentally, but the

above simulations do give some insight into the processes. Two mechanisms are possible: initial hydrogen bond formation into β-sheets and eventual reorganization into the cylinder or initial micelle formation by hydrophobic collapse followed by β-sheet formation then elongation into the cylinder. The simulations show that the path of the self-assembly taken in a particular instance is highly dependent on the initial conditions. In both cases, the nucleation depends on the interplay between the entropy change upon aggregation and the dominant attractive forces, i.e. hydrogen bonding or hydrophobic.

5. Outlook

This review highlights a growing set of codes to control rationally the formation of finite supramolecular assemblies with defined architectures that reach into the molar mass scale of polymers. We have offered examples that demonstrate they are fertile ground to advance soft matter functions. Two specific directions of great promise are their use in electronic and biological functions. We are confident that additional codes for such supramolecular assemblies will emerge in time. An important code under development in our laboratory is the control of pitch in supramolecular helices (Li & Stupp in preparation). The development of many other important codes will require us to identify specific functional targets, and then to proceed for their search with systematic work correlating molecular and assembly structure guided by theory and simulation.

We are grateful for the generous financial support from DOE, NSF, NSF–NSEC and NIH for their financial support. Martin Pralle is acknowledged for the TEM of the G4 dendron, Steve Bull for his solution-phase peptide synthesis and the various co-workers in the Stupp laboratory cited below.

References

Allen, M. P. & Tildesley, D. J. 1987 *Computer simulation of liquids*. Oxford, UK: Oxford Science Publications.

Bain, C. D. & Whitesides, G. M. 1988 Molecular-level control over surface order in self-assembled monolayer films of thiols on gold. *Science* **240**, 62–63. (doi:10.1126/science.240.4848.62)

Behanna, H. A., Donners, J. J. J. M., Gordon, A. C. & Stupp, S. I. 2005 Coassembly of amphiphiles with opposite peptide polarities into nanofibers. *J. Am. Chem. Soc.* **127**, 1193–1200. (doi:10.1021/ja044863u)

Chandler, D. 1978 Statistical-mechanics of isomerization dynamics in liquids and transition-state approximation. *J. Chem. Phys.* **68**, 2959–2970. (doi:10.1063/1.436049)

Estroff, L. A. & Hamilton, A. D. 2004 Water gelation by small organic molecules. *Chem. Rev.* **104**, 1201–1217. (doi:10.1021/cr0302049)

Fields, G. B., Lauer, J. L., Dori, Y., Forns, P., Yu, Y. C. & Tirrell, M. 1998 Proteinlike molecular architecture: biomaterial applications for inducing cellular receptor binding and signal transduction. *Biopolymers* **47**, 143–151. (doi:10.1002/(SICI)1097-0282(1998)47:2<143::AID-BIP3>3.0.CO;2-U)

Hartgerink, J. D., Beniash, E. & Stupp, S. I. 2001 Self-assembly and mineralization of peptide-amphiphile nanofibers. *Science* **294**, 1684–1688. (doi:10.1126/science.1063187)

Hasenknopf, B., Lehn, J. M., Kneisel, B. O., Baum, G. & Fenske, D. 1996 Self-assembly of a circular double helicate. *Angew. Chem., Int. Ed. Engl.* **35**, 1838–1840. (doi:10.1002/anie.199618381)

Hasenknopf, B., Lehn, J. M., Boumediene, N., Dupont-Gervais, A., Van Dorsselaer, A., Kneisel, B. & Fenske, D. 1997 Self-assembly of tetra- and hexanuclear circular helicates. *J. Am. Chem. Soc.* **119**, 10 956–10 962. (doi:10.1021/ja971204r)

Hill, J. P. *et al.* 2004 Self-assembled hexa-peri-hexabenzocoronene graphitic nanotube. *Science* **304**, 1481–1483. (doi:10.1126/science.1097789)

Hoeben, F. J. M. *et al.* 2004 Efficient energy transfer in mixed columnar stacks of hydrogen-bonded oligo(*p*-phenylene vinylene)s in solution. *Angew. Chem. Int. Ed.* **43**, 1976–1979. (doi:10.1002/anie.200353451)

Hof, F., Craig, S. L., Nuckolls, C. & Rebek Jr, J. 2002 Molecular encapsulation. *Angew. Chem. Int. Ed.* **41**, 1488–1508. (doi:10.1002/1521-3773(20020503)41:9<1488::AID-ANIE1488>3.0.CO;2-G)

Huang, Y., Duan, X. F., Wei, Q. Q. & Lieber, C. M. 2001 Directed assembly of one-dimensional nanostructures into functional networks. *Science* **291**, 630–633. (doi:10.1126/science.291.5504.630)

Israelachvili, J. N., Mitchell, D. J. & Ninham, B. W. 1976 Theory of self-assembly of hydrocarbon amphiphiles into micelles and bilayers. *J. Chem. Soc. Farad. Trans. II* **72**, 1525–1568. (doi:10.1039/f29767201525)

Jiang, H., Guler, M. O. & Stupp, S. I. 2007 The internal structure of self-assembled peptide amphiphiles nanofibers. *Soft Matter* **3**, 454–462. (doi:10.1039/b614426h)

Koert, U., Harding, M. M. & Lehn, J. M. 1990 DNH deoxyribonucleohelicates—self assembly of oligonucleosidic double-helical metal-complexes. *Nature* **346**, 339–342. (doi:10.1038/346339a0)

Leach, A. R. 2001 *Molecular modeling. Principles and applications*. New York, NY: Prentice Hall.

Lehn, J. M. 2002 Toward self-organization and complex matter. *Science* **295**, 2400–2403. (doi:10.1126/science.1071063)

Li, L.-S. & Stupp, S. I. In preparation. A molecular torque mechanism to tune pitch in supramolecular helices.

Li, L. M., Beniash, E., Zubarev, E. R., Xiang, W. H., Rabatic, B. M., Zhang, G. Z. & Stupp, S. I. 2003 Assembling a lasing hybrid material with supramolecular polymers and nanocrystals. *Nat. Mater.* **2**, 689–694. (doi:10.1038/nmat983)

Mateos-Timoneda, M. A., Crego-Calama, M. & Reinhoudt, D. N. 2004 Supramolecular chirality of self-assembled systems in solution. *Chem. Soc. Rev.* **33**, 363–372. (doi:10.1039/b305550g)

Messer, B., Song, J. H. & Yang, P. D. 2000 Microchannel networks for nanowire patterning. *J. Am. Chem. Soc.* **122**, 10 232–10 233. (doi:10.1021/ja002553f)

Messmore, B. W. & Stupp, S. I. 2005 Mirror image nanostructures. *J. Am. Chem. Soc.* **127**, 7992–7993. (doi:10.1021/ja051183y)

Messmore, B. W., Hulvat, J. F., Sone, E. D. & Stupp, S. I. 2004 Synthesis, self-assembly, and characterization of supramolecular polymers from electroactive dendron rodcoil molecules. *J. Am. Chem. Soc.* **126**, 14 452–14 458. (doi:10.1021/ja049325w)

Nuzzo, R. G., Fusco, F. A. & Allara, D. L. 1987 Spontaneously organized molecular assemblies. 3. Preparation and properties of solution adsorbed monolayers of organic disulfides on gold surfaces. *J. Am. Chem. Soc.* **109**, 2358–2368. (doi:10.1021/ja00242a020)

Paramonov, S. E., Jun, H. W. & Hartgerink, J. D. 2006 Self-assembly of peptide-amphiphile nanofibers: the roles of hydrogen bonding and amphiphilic packing. *J. Am. Chem. Soc.* **128**, 7291–7298. (doi:10.1021/ja060573x)

Porter, M. D., Bright, T. B., Allara, D. L. & Chidsey, C. E. D. 1987 Spontaneously organized molecular assemblies. 4. Structural characterization of normal-alkyl thiol monolayers on gold by optical ellipsometry, infrared-spectroscopy, and electrochemistry. *J. Am. Chem. Soc.* **109**, 3559–3568. (doi:10.1021/ja00246a011)

Pralle, M. U., Urayama, K., Tew, G. N., Neher, D., Wegner, G. & Stupp, S. I. 2000 Piezoelectricity in polar supramolecular materials. *Angew. Chem. Int. Ed.* **39**, 1486–1489. (doi:10.1002/(SICI)1521-3773(20000417)39:8<1486::AID-ANIE1486>3.0.CO;2-K)

Rajangam, K., Behanna, H. A., Hui, M. J., Han, X. Q., Hulvat, J. F., Lomasney, J. W. & Stupp, S. I. 2006 Heparin binding nanostructures to promote growth of blood vessels. *Nano Lett.* **6**, 2086–2090. (doi:10.1021/nl0613555)

Sayar, M. & Stupp, S. I. 2001 Self-organization of rod-coil molecules into nanoaggregates: a coarse grained model. *Macromolecules* **34**, 7135–7139. (doi:10.1021/ma001400+)

Sayar, M., de la Cruz, M. O. & Stupp, S. I. 2003 Polar order in nanostructured organic materials. *Europhys. Lett.* **61**, 334–340. (doi:10.1209/epl/i2003-00179-4)

Schenning, A., von Herrikhuyzen, J., Jonkheijm, P., Chen, Z., Wurthner, F. & Meijer, E. W. 2002 Photoinduced electron transfer in hydrogen-bonded oligo(*p*-phenylene vinylene)-perylene bisimide chiral assemblies. *J. Am. Chem. Soc.* **124**, 10 252–10 253. (doi:10.1021/ja020378s)

Silva, G. A., Czeisler, C., Niece, K. L., Beniash, E., Harrington, D. A., Kessler, J. A. & Stupp, S. I. 2004 Selective differentiation of neural progenitor cells by high-epitope density nanofibers. *Science* **303**, 1352–1355. (doi:10.1126/science.1093783)

Smith, P. A., Nordquist, C. D., Jackson, T. N., Mayer, T. S., Martin, B. R., Mbindyo, J. & Mallouk, T. E. 2000 Electric-field assisted assembly and alignment of metallic nanowires. *Appl. Phys. Lett.* **77**, 1399–1401. (doi: 10.1063/1.1290272)

Sone, E. D., Zubarev, E. R. & Stupp, S. I. 2002 Semiconductor nanohelices templated by supramolecular ribbons. *Angew. Chem. Int. Ed.* **41**, 1706–1709. (doi:10.1002/1521-3773(20020517)41:10<1705::AID-ANIE1705>3.0.CO;2-M)

Stendahl, J. C., Li, L. M., Zubarev, R., Chen, Y. R. & Stupp, S. I. 2002 Toughening of polymers by self-assembling molecules. *Adv. Mater.* **14**, 1540–1543. (doi:10.1002/1521-4095(20021104)14:21<1540::AID-ADMA1540>3.0.CO;2-T)

Stupp, S. I., LeBonheur, V., Walker, K., Li, L. S., Huggins, K. E., Keser, M. & Amstutz, A. 1997 Supramolecular materials: self-organized nanostructures. *Science* **276**, 384–389. (doi:10.1126/science.276.5311.384)

Sun, W. Y., Yoshizawa, M., Kusukawa, T. & Fujita, M. 2002 Multicomponent metal–ligand self-assembly. *Curr. Opin. Chem. Biol.* **6**, 757–764. (doi:10.1016/S1367-5931(02)00358-7)

Terech, P. & Weiss, R. G. 1997 Low molecular mass gelators of organic liquids and the properties of their gels. *Chem. Rev.* **97**, 3133–3159. (doi:10.1021/cr9700282)

Tew, G. N., Li, L. M. & Stupp, S. I. 1998 Polar and luminescent supramolecular films. *J. Am. Chem. Soc.* **120**, 5601–5602. (doi:10.1021/ja9727732)

Tsonchev, S., Schatz, G. C. & Ratner, M. A. 2003 Hydrophobically-driven self-assembly: a geometric packing analysis. *Nano Lett.* **3**, 623–626. (doi:10.1021/nl0340531)

Tsonchev, S., Troisi, A., Schatz, G. C. & Ratner, M. A. 2004 On the structure and stability of self-assembled zwitterionic peptide amphiphiles: a theoretical study. *Nano Lett.* **4**, 427–431. (doi:10.1021/nl0351439)

Velichko, Y. S., Stupp, S. I. & Olvera de la Cruz, M. In preparation.

Ward, M. D. 2005 Directing the assembly of molecular crystals. *MRS Bull.* **30**, 705–712.

Whaley, S. R., English, D. S., Hu, E. L., Barbara, P. F. & Belcher, A. M. 2000 Selection of peptides with semiconductor binding specificity for directed nanocrystal assembly. *Nature* **405**, 665–668. (doi:10.1038/35015043)

Whitesides, G. M. & Grzybowski, B. 2002 Self-assembly at all scales. *Science* **295**, 2418–2421. (doi:10.1126/science.1070821)

Whitesides, G. M., Mathias, J. P. & Seto, C. T. 1991 Molecular self-assembly and nanochemistry—a chemical strategy for the synthesis of nanostructures. *Science* **254**, 1312–1319. (doi:10.1126/science.1962191)

Whitesides, G. M., Simanek, E. E., Mathias, J. P., Seto, C. T., Chin, D. N., Mammen, M. & Gordon, D. M. 1995 Noncovalent synthesis—using physical–organic chemistry to make aggregates. *Acc. Chem. Res.* **28**, 37–44. (doi:10.1021/ar00049a006)

Yu, Y. C., Tirrell, M. & Fields, G. B. 1998 Minimal lipidation stabilizes protein-like molecular architecture. *J. Am. Chem. Soc.* **120**, 9979–9987. (doi:10.1021/ja981654z)

Zubarev, E. R., Pralle, M. U., Sone, E. D. & Stupp, S. I. 2001 Self-assembly of dendron rodcoil molecules into nanoribbons. *J. Am. Chem. Soc.* **123**, 4105–4106. (doi:10.1021/ja015653+)

Zubarev, E. R., Sone, E. D. & Stupp, S. I. 2006 The molecular basis of self-assembly of dendron-rod-coils into one-dimensional nanostructures. *Chem. Eur. J.* **12**, 7313–7327. (doi:10.1002/chem.200600619)